

A Preventive-Corrective Scheme for Ensuring Power System Security During Active Wildfire Risks

Satyaprajna Sahoo, *Student Member, IEEE*, and Anamitra Pal, *Senior Member, IEEE*

Abstract—The focus of this paper is on operating the electric power grid in a secure manner when wildfire risks are high. This is a challenging problem because of the uncertain ways in which the fires can impact the operation of the power system. To address this challenge, we propose a novel preventive-corrective coordinated decision-making scheme that quickly mitigates both static and dynamic insecurities given the risk of active wildfires in a region. The scheme utilizes a comprehensive contingency analysis tool for *multi-asset outages* that leverages: (i) a “Feasibility Test” algorithm which exhaustively desaturates overloaded cut-sets to prevent cascading line outages, and (ii) a data-driven transient stability analyzer which alleviates dynamic instabilities. This tool is then used to operate a coordinated unit commitment/optimal power flow model that is designed to adapt to varying risk levels associated with wildfires. Depending on the allowed risk, the model balances economical operation and grid robustness. The results obtained using the IEEE 118-bus system indicate that the proposed approach alleviates system vulnerabilities to wildfires while also minimizing operational cost.

Index Terms—Cut-set saturation, Preventive-corrective coordination, Static security, Transient stability, Wildfire

NOMENCLATURE

ΔP_{tr}	Transient stability transfer margin
λ	Generalised wildfire risk in target area
λ_b	Risk metric for post contingency branch overloads
λ_c	Risk metric for cut-set desaturation
λ_N	Risk metric for power flowing through vulnerable lines
λ_t	Risk metric for transient stability correction
$\Delta P_{K_{crit}}$	Transfer margin identified for cut-set K_{crit}
δ	Rotor angle
ϵ	Desired stability margin
η_{us}	Stability margin of the unstable system
κ_{crit}	Set of all identified saturated cut-sets
CM	Set of critical machines
LODF	Line Outage Distribution Factor
NM	Set of non-critical machines
PTDF	Power Transfer Distribution Factor
TSI	Transient Stability Index
τ_n	Linear sensitivity factor
ξ	Contingency List
a_i	Static cost coefficient of generator i
b_i	Linear cost coefficient of generator i
B_r	Set of all branches
c_i	Quadratic cost coefficient of generator i
f_e	Active power flowing in branch e
F_i	Cost function of generator i

G	Set of all generators
G_d	Set of inactive generators
K_{crit}	Identified saturated cut-set
L	Set of all loads
l_j	Active power of load j
M	Inertia coefficient
m_j	Cost of load-shed
p_i^0	Pre-contingency active power produced by generator i
p_i^n	Post-contingency active power produced by generator i
p_i	Active power output of generator i
u_i	Binary variable signifying status of generator i

I. INTRODUCTION

IN recent times, the increasing frequency, intensity, and spread of wildfires has presented significant challenges not only to emergency personnel and forest authorities, but also to the operation of electric power systems. While the impacts on emergency services and forest officials are relatively easier to understand, the interaction between wildfires and the electric power infrastructure is more complex. Power utilities are expected to take measures to prevent initiation of wildfires by their equipment (most often, power lines), while simultaneously operating the grid in a robust and economic manner in the presence of high wildfire risks [1]–[4]. While past research has extensively explored the former issue, this paper focuses on the latter: *ensuring security and stability of the power system in the face of active wildfire risks*.

Analyses of major system interruptions related to wildfires have identified cascading outages resulting from overloaded lines, instabilities caused by frequent arc-faults, and/or preemptive disconnections as the primary cause(s) (for the interruptions). Overloads occur because the heat from ongoing wildfires affect the nearby power lines resulting in *lowering of the conductor’s current carrying capacity* [5]. This lowering can then cause bottlenecks to appear in other parts of the system [6]. Arc-faults are both precursors of grid-initiated wildfires as well as occur when a fire ignited by another source (e.g., lightning) approaches the power lines. Wildfire inducing/induced arc-faults are unique in the sense that they occur *multiple times within a short time-period* [7]. Conventional contingency analysis tools that usually deal with non-repeating faults are not equipped to handle such phenomena. Lastly, *preemptively disconnecting lines bears a very high social cost* [8]. For example, over 2.7 million people were affected during the 2019 California fires when preemptive measures taken by the local utility resulted in more than 940,000 homes and businesses losing electricity [9]. To summarize, it is crucial that both the static security as well as the dynamic stability

This work was supported in part by the National Science Foundation (NSF) grant under Award ECCS-2132904.

Satya Sahoo (email: sssahoo2@asu.edu) is a graduate student, and Anamitra Pal (email: Anamitra.Pal@asu.edu) is an Associate Professor in the School of Electrical, Computer, and Energy Engineering (ECEE) at Arizona State University (ASU).

implications of a potential wildfire contingency are considered for ensuring reliable and resilient power system operation.

While there is significant research aimed at wildfire risk management in the context of the electric power grid [10], these efforts predominantly revolve around risk quantification [11], resilience assessment [12] resource allocation [13], and/or system upgrades [14]. Addressing the unique security and stability challenges posed by wildfires in real-time requires a holistic approach that is currently missing in the state-of-the-art ([5]–[8], [10]–[14]). At the same time, static security assessment and enhancement in the context of storms and hurricanes with the aim of minimizing operational cost and load-shed has been formulated in [15]–[17]. Similarly, a multi-state model for dynamic security enhancement against faults caused by hurricanes was developed in [18]. However, [15]–[18] either assessed stability after contingency manifestation and/or did not explore efficient utilization of the stability results in both the day-ahead and the real-time stages. Specifically, coordination between day-ahead and real-time operations is crucial for achieving robust *and* economic operation when multiple contingencies manifest. Lastly, although prior research has integrated transient stability constraints into an optimal power flow (OPF) problem (called TSCOPF henceforth) [19], [20], or a unit commitment (UC) problem (called TSCUC henceforth) [21], [22], such problems have not been investigated in the presence of active wildfire risks. Moreover, the direct application of TSCOPF/TSCUC to an extreme event scenario (such as wildfire) is not appropriate because of the heightened uncertainty associated with such scenarios as well as the severely limiting nature of the stability constraints.

In light of the above-mentioned realizations, the salient contributions of this paper are outlined as follows:

- A comprehensive contingency analysis tool for wildfire inducing/induced faults is developed to exhaustively analyze *multi-asset outages*, considering the ability of these outages to affect the grid from both static security as well as dynamic stability perspectives.
- The tool first leverages a *Feasibility Test* (FT) [16] algorithm that, given a sequence of outages, is able to quickly and exhaustively identify and correct cut-set¹ saturation. Secondly, the tool has a transient stability analysis component that utilizes machine learning (ML) to analyse and correct rotor angle instabilities caused by multiple frequent arc-faults and line outages.
- This contingency analysis tool is then used to operate a two-stage preventive-corrective coordinated optimization model to optimally allocate resources based on actual system conditions and allowed risk. The preventive component is based on a cut-set and stability constrained UC (CSCUC) that brings additional generators online to support those regions of the system that are at risk of wildfires in the near-future. The corrective component is based on a cut-set and stability constrained OPF (CSCOPF) that quickly redispatches the system given the contingency risk in real-time.

Detailed analyses performed using the IEEE 118-bus system demonstrate that the proposed approach is able to alleviate cascading outages due to static/dynamic insecurities with minimal increase in operational cost.

The rest of the paper is structured as follows. Section II first discusses the impact of wildfires on power system operations, and then proposes two solution methodologies for mitigating the steady-state and transient impacts of such extreme events. Section III integrates these two methodologies into a UC/OPF formulation to create a coordinated decision-making framework that considers the risk of a wildfire event in the region for optimally operating the system. Section IV analyses the results obtained on implementing the proposed model on an identified vulnerable transmission corridor of the test system (the IEEE 118-bus system). The conclusions are drawn in Section V.

II. STRATEGIES TO MITIGATE IMPACTS OF MULTI-ASSET OUTAGES DURING WILDFIRES

A. Problem Scope

Wildfires and their interaction with the electric power infrastructure constitute a multi-faceted problem. Grid-initiated fires are usually the result of high-impedance faults that: (a) occur under environmental conditions that are conducive for a faster spread, (b) are harder to detect, and (c) happen in quick succession [23]–[26]. The fear is so severe that utilities are often forced to change their protection settings apriori (say, a day before) in anticipation of high wildfire risks. For fires started by another source and approaching the power lines: (a) the spatio-temporal process of wildfire spread is based on the local climate and geography (topography, vegetation, wind); (b) the breakdown mechanisms of the air gap around the lines vary with time, location, and wildfire proximity and intensity; (c) the outcomes can range from multiple arcing events to a complete line melt-down (permanent outage) [27]–[29]. A variety of tools already exist for tracking wildfire spread over different geographical regions (e.g., FlamMap [30]). Therefore, this study assumes that the risk of a wildfire affecting a target area is known apriori (e.g, a day in advance).

To prevent starting a grid-initiated wildfire when the environmental conditions are ripe, power utilities had previously resorted to an intervention policy called *public safety-power shutoffs* (PSPS). However, PSPS resulted in a much larger portion of the populace to lose electricity [31]. Similarly, without knowledge of the environmental conditions around a power line when a fire is nearby, it is not possible to determine the air quality and/or the type of outcome that might occur (frequent multiple arc-faults to permanent outage). In this regard, one strategy could be to assume that all power lines located in an active wildfire area are preemptively de-energized, and then solve an optimal generation redispatch problem in presence of topology changes [32]. However, as explained in [8], such a strategy is not optimal from a socio-techno-economic perspective. Therefore, this study is aimed at striking a balance between economical operation and grid robustness by pre-allocating resources in the day-ahead stage and reallocating them, if need be, in real-time.

¹A cut-set is a set of lines, which if tripped, would create disjoint islands in the network. Therefore, saturated/overloaded cut-sets are the most vulnerable interconnections of the system as they have limited power transfer capability.

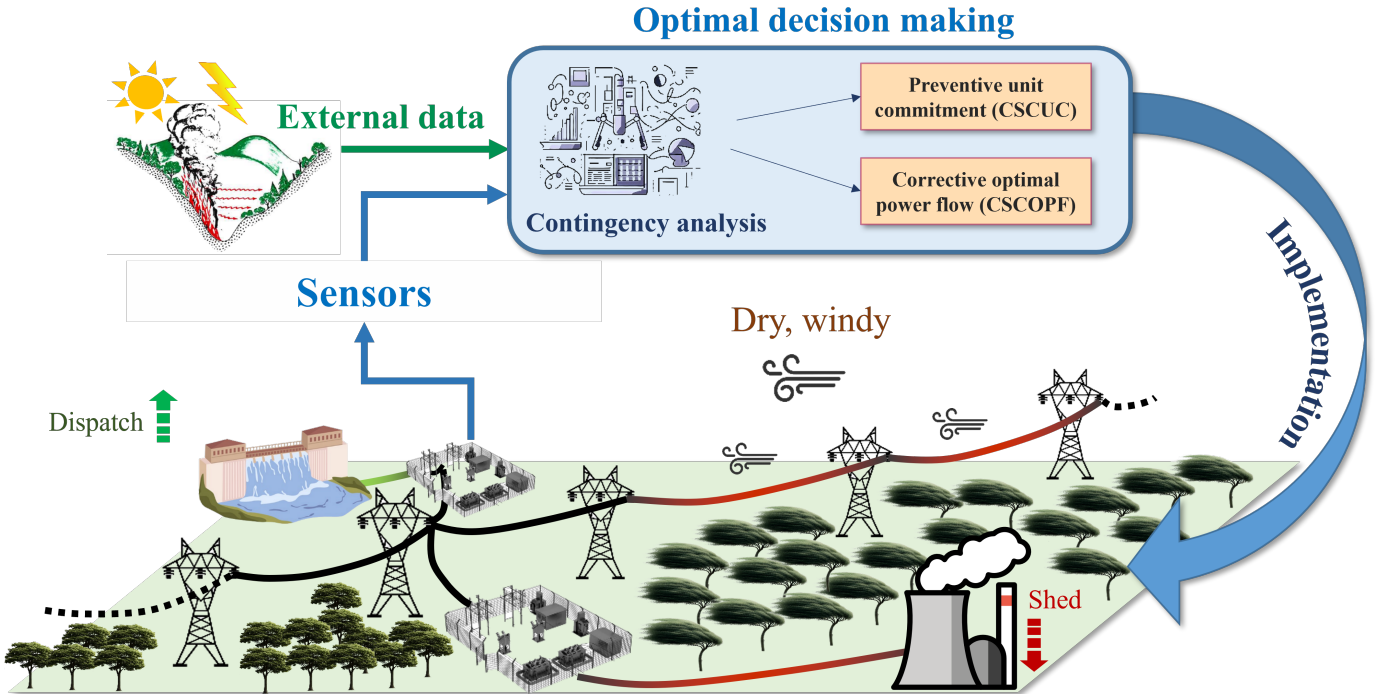


Fig. 1: Overview of the proposed preventive-corrective coordinated action scheme.

We now outline two power system vignettes that exemplify the scope of the methodology developed in this paper:

Vignette 1: The risk of wildfire is high for the next day in a particular region but the fire has not started yet, and the power utility wants to pre-allocate/reallocate resources so as to secure the system without preemptively deenergizing all the power lines in that region.

Vignette 2: A fire is burning in a neighboring region, and there is a high probability of the fire spreading to the region-under-study on the following day. In this case, the utility wants to pre-allocate/reallocate resources so that the system runs in a secure and stable manner while considering the dynamic nature of wildfire risks.

An illustration of the implementation of the proposed preventive-corrective coordinated action scheme is given in Fig. 1. In the pre-contingency stage, a contingency analysis is performed on the high-risk areas (dry, windy), following which power flowing through that region is lowered and additional generators are brought online in other regions (indicated by red and green arrows). In the real-time stage, the online generators are optimally redispatched to quickly and economically steer the system to a secure and stable state.

Lastly, note that the proposed formulation is generic and, with suitable modifications, can be used to tackle other extreme events/multi-asset outage causing contingencies. The focus of this paper, however, is on wildfires. In the following sub-section, we highlight the FT algorithm and the ML-based transient stability analysis which form the backbone of the proposed comprehensive contingency analysis tool for combating active wildfire risks.

B. Feasibility Test (FT)-based Cut-set Security Analysis

Since wildfires generally impact more than one line in a target area, their outage can lead to a load-generation mismatch in areas that are connected by those lines. Cut-sets, by definition, are the set of lines that join two areas. Therefore, by detecting and alleviating saturated cut-sets, security criteria during multiple line losses can be strengthened. A saturated cut-set is one whose aggregate power flow exceeds the limits of the lines that form the cut-set. This is mathematically described by:

$$\sum_{\forall e \in K_{\text{crit}}} f_e > \sum_{\forall e \in K_{\text{crit}}} f_e^{\text{max}} \quad (1)$$

where, f_e^{max} is the maximum power flow allowed through the e^{th} line of the saturated cut-set, K_{crit} . By exploiting the principle that the cut-set power flow is not impacted by the method employed to redirect the power flowing through a line that faces an outage [15], a fast and scalable algorithm called FT was developed that exhaustively identifies and alleviates all saturated cut-sets for a given contingency [16]. The identified cut-sets can be desaturated by reducing the aggregate power flowing through the constituent lines. This is mathematically expressed as:

$$\sum_{\forall e \in K_{\text{crit}}} \Delta f_e \leq -\Delta P_{K_{\text{crit}}} \quad \forall K_{\text{crit}} \in \kappa_{\text{crit}} \quad (2)$$

where, $\Delta P_{K_{\text{crit}}}$ is the required transfer margin for K_{crit} , and indicates the total amount of power that must be reduced across the lines of K_{crit} to prevent it from being overloaded. More details about the FT algorithm and its capabilities can be found in [15], [16].

C. Machine Learning (ML)-based Transient Stability Analysis

Multiple arc-faults during periods of high wildfire risks and cascading outages caused by ongoing wildfires possess the ability to cause transient instability in the form of rotor angle instabilities in the synchronous generators present in the system. Transient stability (rotor angle stability) is assessed from the difference in the maximum rotor angle (δ_{\max}) between two consecutive synchronous machines. The metric used to analyze transient stability under such situations, called the transient stability index (TSI), is mathematically defined by:

$$\text{TSI} = \frac{360 - \delta_{\max}}{360 + \delta_{\max}} \times 100 \quad (3)$$

The system is stable if $\text{TSI} > 0$, and unstable otherwise. An unstable system is characterized by at least one generator losing synchronism, and eventually tripping. For an unstable contingency, the total generation can be classified into stable and unstable generators, with the stable generators being those whose rotor angles are below δ_{\max} . Given a contingency that leads to transient instability, the instability can be corrected using the integrated extended equal area criterion (IEEAC) [33]. The theory of the IEEAC stipulates that transferring requisite amount of generation from the unstable generators (CM) to the stable generators (NM) can make the TSI positive. The required amount of generation that must be shifted is given by [34]:

$$\Delta P_{tr} \geq \left(\frac{-\eta_{us} + \epsilon}{\tau_n} \right) \cdot \left(\frac{M}{M_{CM}} + \frac{M}{M_{NM}} \right)^{-1} \quad (4)$$

where, M , M_{CM} , and M_{NM} are the one machine infinite bus (OMIB) inertia coefficients of the whole system, CM, and NM, respectively, and $CM \cup NM = G$. ΔP_{tr} is referred to as the transient stability correction factor (TSCF). Eq. (4) can be used to provide a transient stability constraint as shown below:

$$\sum_{\forall i \in CM} \Delta p_i \leq -\Delta P_{tr} \quad (5)$$

Now, the calculation of ΔP_{tr} requires performing multiple time domain simulations (TDSs) for a single contingency, which is computationally expensive to do in real-time when the list of potential contingencies is large. Furthermore, one must also consider the variability of the loads - a factor that will be compounded if solar or wind is present. To account for both of these factors, we exploit the quasi-linear relationship between the pre-contingency one machine mechanical power and the transient stability margin [33]. Specifically, we posit that a quasi-linear relationship exists between the TSCF and the pre-contingency loading condition (l), since the pre-contingency mechanical power is linearly related to the loads. Consequently, we formulate a linear regression model that estimates the required TSCF for a forecasted loading condition, as shown below [34]:

$$\Delta \hat{P}_{tr} = \sum_{i \in L} \theta_i l_i + \theta_0 = \Upsilon(l_i) \quad (6)$$

$$J(\theta) = \frac{1}{k} \sum_{i=1}^k (\Delta \hat{P}_{tr_i} - \Delta P_{tr_i})^2 \quad (7)$$

where, θ are the weights, $J(\theta)$ is the loss function, and k is the batch size. This data-driven model for estimating the TSCF is referred to as the transient stability constraint prediction (TSCP) algorithm, and is denoted by Υ . The ability of different ML techniques in estimating ΔP_{tr} is compared in Section IV-A. More details about the TSCP algorithm and its implementation can be found in [34].

With the FT algorithm and the ML-based transient stability analysis generating appropriate constraints, the goal is now to integrate them into the UC/OPF problem to achieve secure and stable power system operation during active wildfire risks, while also being economical. This goal is achieved through the preventive-corrective coordinated action scheme described in the next section.

III. PREVENTIVE-CORRECTIVE COORDINATION

In the day-ahead stage, the conventional UC formulation helps to find a low-cost operating schedule for the generators. However, it can be suitably *modified* to better prepare the system for extreme events. Similarly, the corrective actions of a *modified* OPF formulation can minimize (if not eliminate) the impact of contingencies by quickly reducing the power flowing through the more vulnerable areas in real-time. Together, this coordinated preventive-corrective decision-making scheme can rapidly, safely, and economically steer the power system towards a secure and stable state. The following subsections describe how such a scheme can be developed and implemented for managing active wildfire risks.

A. Preventive Unit Commitment (UC)

In the preventive stage, previously inactive generators are brought online to prepare the system for a contingency that might occur in the near-future. Note that although the generators are brought online, they may or may-not dispatch in real-time (this decision is made in the next sub-section). Hence, we formulate a *modified* UC problem as described below. We start by expressing the generator costs (F_i) as a quadratic function of the output power (p_i):

$$F_i(p_i) = a_i + b_i p_i + c_i (p_i)^2 \quad (8)$$

Since the proposed formulation is modeled as an optimal rescheduling problem, the cost of change in generation can be simplified to:

$$\begin{aligned} \Delta F_i(\Delta p_i) &= \{a_i + b_i p_i^n + c_i (p_i^n)^2\} \\ &\quad - \{a_i + b_i p_i^0 + c_i (p_i^0)^2\} \\ &= c_i (\Delta p_i)^2 + (b_i + 2c_i p_i^0) \Delta p_i \end{aligned} \quad (9)$$

where, the superscripts 0 and n refer to the pre-contingency and post-contingency status, respectively, of the corresponding variable, and $\Delta p_i = p_i^n - p_i^0$. The overall objective should include the cost of generation change and load shed while also considering the availability of inactive generators. Now, the UC decisions are based on the post-contingency operation (which generators are most economical after the vulnerable assets are out), hence only the generators that are currently inactive are considered in the modified UC. This decreases the number of binary variables in the proposed formulation

by a considerable amount. Taking all of this into account, the desired objective function can be written as:

$$\min_{\Delta p_i, \Delta l_j, u_i} \sum_{\forall i \in G} (c_i \Delta p_i^2 + d_i \Delta p_i) + \sum_{\forall j \in L} (m_j \Delta l_j) + \sum_{\forall i \in G_d} u_i a_i \quad (10)$$

where, $d_i = (b_i + 2c_i p_i^0)$. The set of inactive generators G_d is a subset of G . Load shed cost m_j is chosen to be higher than the generator costs, to de-incentivize power outage. The binary variable u_i is used to bring additional generators online considering the post-contingency situation, including the assets out of service due to the contingency. The overall objective is now subjected to the following constraints:

$$u_i \cdot (p_i^{\min} - p_i^0) \geq \Delta p_i \geq u_i \cdot (p_i^{\max} - p_i^0) \quad \forall i \in G \quad (11)$$

$$u_i = 1 \quad \forall i \in \{G - G_d\} \quad (12)$$

$$l_j^{\min} - l_j^0 \geq \Delta l_j \geq l_j^{\max} - l_j^0 \quad \forall j \in L \quad (13)$$

$$f_e^{\min} - f_e^0 \leq \sum_{\forall i \in G} \text{PTDF}_{e,i}^r \Delta p_i - \sum_{\forall j \in L} \text{PTDF}_{e,j}^r \Delta l_j \leq f_e^{\max} - f_e^0 \quad \forall e \in B_r \quad (14)$$

$$\sum_{\forall i \in G} \Delta p_i = \sum_{\forall j \in L} \Delta l_j \quad (15)$$

$$\begin{aligned} & \sum_{\forall i \in G} (\text{PTDF}_{e,i}^r + \text{LODF}_{e,k} \text{PTDF}_{k,i}^r) \Delta p_i \\ & - \sum_{\forall j \in L} (\text{PTDF}_{e,j}^r + \text{LODF}_{e,k} \text{PTDF}_{k,j}^r) \Delta l_j \\ & \leq f_e^{\max} - f_e^0 + (\text{LODF}_{e,k} f_k^0) \quad \forall e, k \in B_r, \xi \end{aligned} \quad (16)$$

$$\begin{aligned} & \sum_{\forall i \in G} (\text{PTDF}_{e,i}^r + \text{LODF}_{e,k} \text{PTDF}_{k,i}^r) \Delta p_i \\ & - \sum_{\forall j \in L} (\text{PTDF}_{e,j}^r + \text{LODF}_{e,k} \text{PTDF}_{k,j}^r) \Delta l_j \\ & \geq f_e^{\min} - f_e^0 + (\text{LODF}_{e,k} f_k^0) \quad \forall e, k \in B_r, \xi \end{aligned} \quad (17)$$

$$\begin{aligned} & \sum_{\forall i \in G} \left(\sum_{\forall u \in K_{\text{crit}}} \text{PTDF}_{u,i} \right) \Delta p_i \\ & - \sum_{\forall j \in L} \left(\sum_{\forall u \in K_{\text{crit}}} \text{PTDF}_{u,j} \right) \Delta l_j \\ & \leq -\Delta P_{K_{\text{crit}}} \quad \forall K_{\text{crit}} \in \kappa_{\text{crit}} \end{aligned} \quad (18)$$

$$\sum_{\forall i \in \text{CM}} \Delta p_i \leq -\Delta P_{tr} \quad (19)$$

Eqs. (11)-(14) provide limits for the optimization variables. Note that the binary variable u_i is set to 1 for the already dispatched generators; this is indicated by (12). The power balance constraint is shown in (15). The post-contingency $N - 1$ branch overload constraints are expressed in (16)-(17). The post-contingency cut-set constraint is modeled in (18), while (19) denotes the transient stability constraint. This completes the description of the modified UC, which is henceforth referred to as the CSCUC.

Algorithm 1 describes the implementation of CSCUC. In the day-ahead stage, a list of contingencies are obtained, and contingency analysis is done with each list using TDS. If a contingency is found to cause transient instabilities or cut-set saturation, then the required transfer margins are calculated, and the TSCP is trained. This is followed by the CSCUC, which recommends additional generators to be brought online in anticipation of the contingency manifesting the next day.

Algorithm 1 CSCUC Implementation

Input: Historical load distributions, Contingency list ξ

Output: Unit Commitment (UC) status u_i

Day-ahead:

- 1: Perform random sampling from the historical load distributions to determine potential loading conditions Ξ
 - 2: Define empty list of constraints Φ
 - 3: **for** loading condition in Ξ **do**
 - 4: Perform TDS using ξ
 - 5: **if** violations detected **then**
 - 6: Generate transient stability constraint using (4)
 - 7: Update Φ
 - 8: **end if**
 - 9: **end for**
 - 10: Train Υ using Φ
 - 11: Run FT to generate constraint (18)
 - 12: CSCUC: Set objective (10)
 - 13: Set constraints (11)-(19)
 - 14: Solve to get UC status, u_i
-

B. Corrective Optimal Power flow (OPF)

In real-time, the rescheduling must be done according to the updated forecasts and contingency risk. By quantifying the risk of a wildfire affecting the region, we can use it to relax constraints (16)-(19) which may be too limiting otherwise, to solve a modified OPF problem (called the CSCOPF problem) and get the desired redispatch. The modified objective is now expressed as:

$$\begin{aligned} \min_{\Delta p_i, \Delta l_j} & \sum_{\forall i \in G} (c_i \Delta p_i^2 + d_i \Delta p_i) + \sum_{\forall j \in L} (m_j \Delta l_j) \\ & + \lambda_c \left(\sum_{\forall i \in G} \sum_{\forall u \in K_{\text{crit}}} \text{PTDF}_{u,i} \Delta p_i \right. \\ & \left. - \sum_{\forall j \in L} \sum_{\forall u \in K_{\text{crit}}} \text{PTDF}_{u,j} \Delta l_j + \Delta P_{K_{\text{crit}}} \right) \\ & + \lambda_t \left(\sum_{\forall i \in \text{CM}} \Delta p_i + \Delta P_{tr} \right) + \lambda_N \left(\sum_{\forall e \in \xi} f_e^2 \right) \end{aligned} \quad (20)$$

In (20), the constraint penalties λ_c and λ_t are representative of the wildfire risk in the target area, and can be varied appropriately to enforce compliance of the cut-set and transient stability constraints. The above-mentioned objective is now subjected to the following constraints, which are similar to those specified for the CSCUC with the additional inclusion of the constraint penalties:

$$p_i^{\min} - p_i^0 \geq \Delta p_i \geq p_i^{\max} - p_i^0 \quad \forall i \in G \quad (21)$$

$$l_j^{\min} - l_j^0 \geq \Delta l_j \geq l_j^{\max} - l_j^0 \quad \forall j \in L \quad (22)$$

$$\begin{aligned} f_e^{\min} - f_e^0 &\leq \sum_{\forall i \in G} \text{PTDF}_{e,i}^r \Delta p_i - \sum_{\forall j \in L} \text{PTDF}_{e,j}^r \Delta l_j \\ &\leq f_e^{\max} - f_e^0 \quad \forall e \in B_r \end{aligned} \quad (23)$$

$$\sum_{\forall i \in G} \Delta p_i = \sum_{\forall j \in L} \Delta l_j \quad (24)$$

$$\begin{aligned} &\sum_{\forall i \in G} (\text{PTDF}_{e,i}^r + \text{LODF}_{e,k} \text{PTDF}_{k,i}^r) \Delta p_i \\ - &\sum_{\forall j \in L} (\text{PTDF}_{e,j}^r + \text{LODF}_{e,k} \text{PTDF}_{k,j}^r) \Delta l_j \quad (25) \\ &\leq \lambda_b (f_e^{\max} - f_e^0 + (\text{LODF}_{e,k} f_k^0)) \quad \forall e, k \in B_r, \xi \end{aligned}$$

$$\begin{aligned} &\sum_{\forall i \in G} (\text{PTDF}_{e,i}^r + \text{LODF}_{e,k} \text{PTDF}_{k,i}^r) \Delta p_i \\ - &\sum_{\forall j \in L} (\text{PTDF}_{e,j}^r + \text{LODF}_{e,k} \text{PTDF}_{k,j}^r) \Delta l_j \quad (26) \\ &\geq \lambda_b (f_e^{\min} - f_e^0 + (\text{LODF}_{e,k} f_k^0)) \quad \forall e, k \in B_r, \xi \end{aligned}$$

The CSCOPF problem formulated above utilizes the status of the generators calculated in the CSCUC as inputs. This ensures that the resulting redispatch is fast as well as economical. The values of the constraint penalties, denoted by $\Lambda = [\lambda_b \ \lambda_c \ \lambda_t \ \lambda_N]$ which constitute the real-time wildfire risk, may be obtained from predictive models using external factors such as weather data [35], or from grid-edge devices monitoring for faults or smoke [36]; it may also be set manually from operator experience. Furthermore, its value may be altered in real-time to shift the system to a more alert state or less alert state depending upon the probability of wildfire in the region-under-study.

Algorithm 2 describes the implementation of CSCOPF. It takes inputs from various sources, including the trained TSCP Υ , and the allowed wildfire risk, Λ . The warm start solution p_i^0 may be obtained from the real-time power injections (which can be estimated [37]) and the load forecasts. Once the risk metrics are set, CSCOPF is run, and the resulting solution is checked for any additional violations using FT and a single TDS. As one approaches the most vulnerable hours of the day, the value of Λ should be increased to better prepare the system for facing the wildfire contingency.

IV. RESULTS

The proposed formulation is tested on the publicly available IEEE 118-bus system. The system consists of 118 buses, 54 generators, and 99 loads. This system is known to be very robust and stable against line outages, so the effects of simulated wildfires in this system emphasizes the true effects of the damage an unmitigated approach can have. For generating diverse operating conditions, equivalent loads from the publicly available 2000-bus synthetic Texas system [38] are first found, and then their variations were captured using kernel density estimation (KDE). The variations in some of the loads are shown in Fig. 2. Random sampling was then performed from the KDEs to generate ≈ 28000 samples of real power load l_i . These loading conditions were then used to perform

Algorithm 2 CSCOPF Implementation

Input: Units committed u_i , Real-time power injections, Real-time wildfire risk Λ , Transient stability analyser Υ
Output: optimal redispatch Δp_i , and load shed Δl_j
Real-time:

- 1: Obtain or set risk λ
- 2: Define empty list of constraints Φ
- 3: Obtain real-time power injection information
- 4: Generate cut-set constraint using (18)
- 5: Generate transient stability constraint using Υ ; see (19)
- 6: Update Φ with constraints (18) and (19)
- 7: **while** additional violations detected **do**
- 8: CSCOPF: Define objective (20) using Φ , apply constraints (21)-(26)
- 9: Solve CSCOPF to get Δp and Δl
- 10: Update dispatch and run power flow
- 11: Run FT and single TDS on updated dispatch
- 12: **if** violations detected **then**
- 13: Update Φ and Go to Step 8
- 14: **end if**
- 15: **end while**

contingency analysis using TDS. The TDSs were performed in PSSE[®], while the two-stage optimization was modeled and solved using Gurobi and Pandapower in Python 3.11.

A common theme across Vignettes 1 and 2 is the possibility of a wildfire impacting a region of the power system in the near-future (e.g., the next day). Accordingly, a prospective transmission corridor comprising two lines (namely, 23 – 25 and 26 – 30) of the 118-bus system was identified, and it was assumed that on the following day, a set of five arc-faults would occur consecutively over a period of three seconds at the end of which each line would suffer a permanent outage. The corrective action analysis used to generate the power shift required in (5) for all the loading conditions were then calculated, and Υ was trained, with the train to test split in the ratio 80 : 20. For obtaining the results shown in the next four sub-sections, the constraint penalties/risk metrics were made to obey the following relation: $\lambda_b = \lambda_c = \lambda_t = \lambda_N * 0.01 = \lambda$; this condition was relaxed in Section IV-E. Note that λ_N

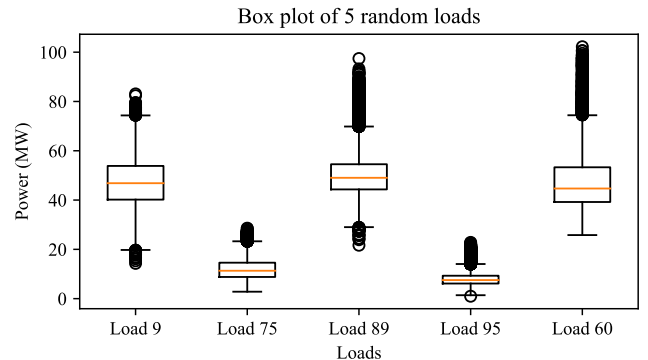


Fig. 2: Load variation data for five loads in the 118-bus system

includes a normalising factor as the associated term is of the unit MW^2 . All computational analyses done in this paper were performed using a computer with an Intel Core (TM) i7-11800H CPU @2.3GHz with 16GB of RAM and an RTX 3070Ti GPU.

A. Contingency Alleviation Actions

The cut-set and transient stability constraints generated for this extreme event scenario is detailed in Table I. The constraints also define the instability alleviation actions, namely, the dispatch of the critical generators (25, 26) must be reduced by at least 118 MW, and the aggregate power flow across the lines (26 – 30, 25 – 27) must be reduced by at least 187 MW. Note that the required rescheduling is considerably large, implying that the alleviation will be subject to ramp-rate constraints. Furthermore, such a large change does lead to additional security violations for the test system, which are captured by the FT algorithm. For these (as well as economic) reasons, it is essential that a coordinated strategy involving both day-ahead and real-time control are employed instead of entrusting everything to real-time corrections.

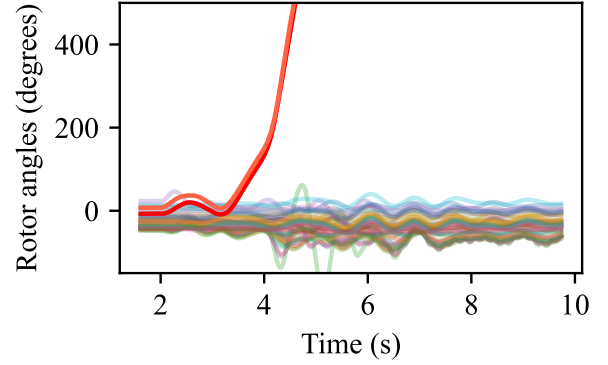
TABLE I: Contingency Impacts

System	118-bus system
Lines tripped	(23-25, 26-30)
N – 1 branch overloads identified	(8-5)
Saturated cut-sets	(26-30, 25-27)
$\Delta P_{K_{crit}}$	187.086 MW
% of capacity	42.51%
Critical Machines (CM) for transient stability	25, 26
ΔP_{tr}	118 MW
Total capacity of tripped generation	534 MW
% of capacity	22.1%

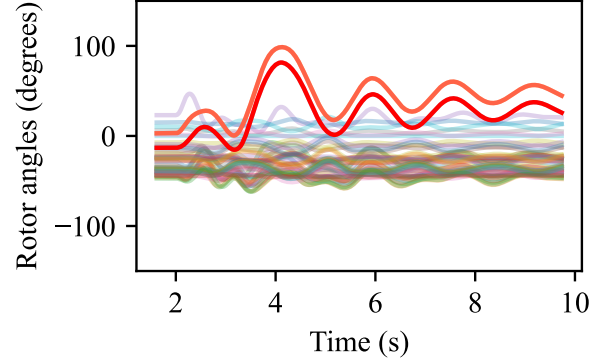
For the contingency-under-investigation, the proposed contingency analysis tool was able to quantify the impacts (of the contingency) as well as determine the actions that must be taken to alleviate them. As an example, Fig. 3 illustrates the transient stability (rotor angles) of two TDSs for this contingency before and after implementing the recommended alleviation actions. The unstable generators (25, 26) are able to ride-through the contingencies and do not lose synchronism after the corrections are applied (compare the red and orange-colored curves in this figure).

The results for the TSCP algorithm, Υ , is given in Table II. In this study, Υ trained using a linear regression model is compared with other data-driven models including ridge regression, support vector regression (SVR) with a radial basis function (RBF) kernel, XGBoost, random forest, elastic net, k -nearest neighbor (KNN), decision tree, and least absolute shrinkage and selection operator (LASSO) regression. The metrics used to gauge the performance of these models include the root mean squared error (RMSE), R^2 score, mean bias deviation (MBD), and R^2 robustness. Note that MBD is a representation of the average bias in the model predictions, and is mathematically defined as:

$$MBD = \frac{\sum_n (y - \hat{y})}{n} \quad (27)$$



(a) TDS without control



(b) TDS with control

Fig. 3: Rotor angle stability for the 118-bus system

Ideally, MBD should be 0, to prevent bias in estimation. However, for the identified problem, underestimation of TSCF (positive MBD) is much worse than overestimation, as the latter leads to uneconomical operation, while the former leads to transient instabilities and the eventual tripping of generators. Therefore, data-driven models that give a *small negative* value for MBD are better. Finally, since load forecasts are naturally subject to errors, it is important to also consider the robustness drop in R^2 , which is calculated by introducing noise into the forecasts and observing the subsequent change in the R^2 score. Naturally, a smaller value of R^2 robustness is preferred.

TABLE II: TSCP Results for Different Data-driven Models

Model	RMSE (MW)	R^2	MBD	R^2 Robustness
Linear Regression	0.31	0.98	$-0.57e-4$	0.0024
Ridge Regression	0.31	0.98	$-0.57e-4$	0.0027
SVR	0.42	0.97	0.02	0.0028
XGBoost	0.94	0.85	-0.004	0.0035
Random Forest	1.51	0.61	0.005	0.0031
Elastic Net	2.13	0.22	$-0.93e-4$	-0.0003
KNN	2.21	0.16	0.58	-0.0004
Decision Tree	2.33	0.06	0.002	-0.0051
LASSO Regression	2.34	0.06	$-0.28e-4$	0.0001

It is clear from the table that linear regression has a low error with a high degree of confidence, even in the presence of noise in the forecasts. This result confirms our earlier

stipulation that a quasi-linear relationship exists between the pre-contingency loading conditions and the transfer margin (see Section II-C). Moreover, the shallow model (linear regression) combined with the interpretable nature of the constraints ensures transparency, i.e., should prevailing conditions shift, a power system operator possesses the discretion to intervene at any stage of the implementation, allowing the application of custom solutions derived from their experience.

B. Day-ahead Unit Commitment

The contingency analysis results shown in Table I are now used for optimal decision-making. In anticipation of a wildfire impacting the identified transmission corridor of the 118-bus system in the following day, the proposed modified UC is performed to determine and dispatch additional generators. The CSCUC is solved assuming the contingency has already manifested, and in the post-contingency state, the committed generators are to be dispatched. The results obtained are shown in Table III. The CSCUC recommends bringing an additional generator online at bus 6. Note that this generator may not dispatch during the times of the day when the risk of fire is low. However, it is cheaper and faster (as shown later in Section IV-D) to bring the system to a ready state with this generator in-service when the risk of wildfire is high (Vignette 1) or the fire enters the region-under-study (Vignette 2).

TABLE III: CSCUC Results

Parameter	Value
Contingency List	[(23-25), (26-30)]
Number of additional generator(s) committed	1
Generator(s) committed	Generator at bus [6]
Total objective (\$/hr)	665.31
Time to solve (s)	0.596

C. Real-time Optimal Redispatch

The optimal reschedule primarily depends on the current status of the wildfire: whether it actually occurs in case of Vignette 1/enters the region-under-study in case of Vignette 2, or it has not impacted the region-under-study yet but the risks continue to be high. It also depends on how alert the power system operator wants the system to be (i.e., the level of allowed risk specified by λ). In the case when a fire is in the region-under-study, the CSCOPF solution is obtained by solving (10) with the values of u_i set based on the day-ahead CSCUC. In the case when a fire has not started but the risks are high, the risk-based formulation given in (20) allows the system to increase its readiness to the contingency gradually (e.g., by increasing λ).

In the following, we consider the latter case in which the fire has not started in the region-under-study of the 118-bus system but the risks remain high. A reschedule of the generators based on $\lambda = 5$ is shown in Fig. 4. In the figure, the blue bars indicate generators that take on additional generation, while the red bars indicate generators that lower their active generation. The major reduction in generation is seen in generators which are directly affected by the contingency-under-consideration, and CSCOPF reschedules them economically while maintaining the security of the rest of the system.

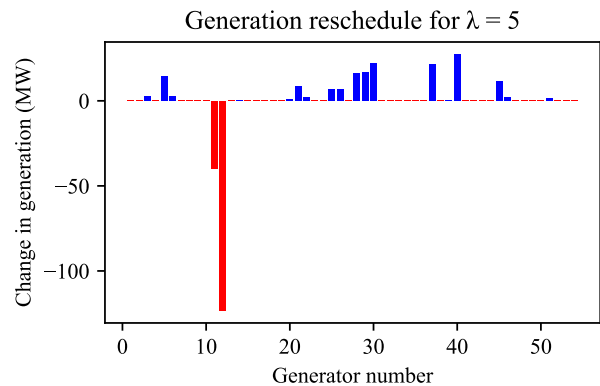


Fig. 4: CSCOPF result: Generator reschedule. Blue generators take on additional generation, while red generators lower their dispatch

D. Comparison with State-of-the-Art

A comparison of the proposed model with the conventional real-time security constrained economic dispatch (RT-SCED) and TSCOPF models is performed for the identified contingency in the 118-bus system, and the results are shown in Table IV. Note that the RT-SCED model has no cut-set or stability constraints, while the TSCOPF has no cut-set constraints. For this comparison, the CSCOPF is solved without any constraint relaxations. That is, this corresponds to a case where the fire is already in the region-under-study. The table shows that while TSCOPF was able to alleviate the stability constraint, it did not alleviate the cut-set insecurities. Meanwhile, RT-SCED increased the cut-set saturation, making the region even more vulnerable. Conversely, the proposed CSCOPF is able to alleviate both vulnerabilities, resulting in a secure solution without resorting to any load shed.

The solution time of CSCOPF is similar to RT-SCED and one-fourth of TSCOPF, implying that the additional constraints do not significantly increase the computational burden of the optimization, with the data-driven transient stability analyzer actually improving the speed of online operation. Economically, CSCOPF has an additional operational cost of about \$1727.48/hr. For context, a system with no control/an insecure solution would have put about 534 MW of generation at risk of tripping which would have led to a loss in revenue of at least \$12,651.44/hr, calculated on the generation side. Lastly, although load-shed was not required for the contingency-under-study, it is important to incorporate it in the problem formulation as a different contingency may require both generation redispatch as well as load-shed.

TABLE IV: Comparative Analysis of CSCOPF Results

Result	RT-SCED	TSCOPF	CSCOPF
CM generation shed (MW)	20.4	118	269.79
Cut-set desaturation (MW)	-131.80	57.519	187.087
Total load shed (MW)	0	0	0
Transient stable	No	Yes	Yes
Cut-set secure	No	No	Yes
Time to solve (s)	0.066	0.256	0.066
Cost (\$/hr)	126,459.97	126,222.28	128,187.95

Next, the importance of a two stage preventive-corrective coordinated approach is demonstrated; the results are shown in Table V. In the table, three cases of the proposed coordinated approach with different levels of risk is compared with a stand-alone real-time CSCOPF solution [34]. While the proposed solution leads to increased start-up costs due to the dispatch of an additional generator (at bus 6), the costs are recovered through lower price of real-time operation.

TABLE V: Two-stage Coordination Results

Additional resources	CSCOPF	CSCUC+CSCOPF (Two-stage)		
		$\lambda=0.1$	$\lambda=5$	$\lambda=7$
Generators committed	0	1	1	1
Start up cost (\$)	0	80	80	80
Real-time cost (\$/hr)	9254.09	6387.75	6756.31	6971.56

E. Sensitivity Analysis

This sub-section explores the flexibility in implementation of the proposed model under the identified problem scope for the region-under-study of the 118-bus system. The primary purpose is to understand the full scale of its applicability and simultaneously, its limitations. To do this, we evaluate the performance of the proposed two-stage optimization formulation by varying λ , i.e, for varying wildfire risk situations. The results are shown in Table VI. For a small λ , economical dispatch is preferred, while the vulnerability of the system to contingencies is high, as it would take a longer amount of time for the critical generators to ramp down to stable levels of generation. For reference, one dispatch cycle is considered in this case to be 15 minutes. Meanwhile by increasing λ , the model prefers clearing these constraints, and hence the risk of the system being affected by a wildfire reduces significantly, albeit at a higher operational cost indicated by the higher (positive) value of the CSCOPF objective.

TABLE VI: Preventive-Corrective Results for Varying λ

Property	$\lambda = 0.1$	$\lambda = 5$	$\lambda = 7$
Power shed in vulnerable lines (%)	12.52	14.95	16.32
CM generation shed (%)	14.78	89.07	117.35
Cut-set desaturation (%)	11.46	33.12	40.86
Total load shed (MW)	0	0	0
CSCOPF objective	-394.59	707.86	994.34
# dispatch cycles to clear constraints	2	1	0

A sensitivity analysis for the most important individual risks is explored next. The sensitivities for the risk metric λ_c and λ_t are shown in Figs. 5 and 6, respectively. In both the figures, the identified vulnerable regions are the regions where the system may be operated at if the wildfire has not manifested yet, for economic reasons, as reducing vulnerability is associated with an almost equivalent increase in cost. These analyses have different effects based on the problem scope. For situations of active wildfire risks in which the contingency has not manifested yet, but the risk is very much present, the system may be run in the vulnerable regions of Figs. 5 and 6. For example, a recommended solution is to set $\lambda_c = 0.3$ and $\log(\lambda_t) = 0.4$, as it results in a reasonable trade-off between operational cost and system vulnerability. On the contrary, if there is a fire in the region-under-study, the system must be

operated beyond the vulnerability regions for both the risk metrics since the affected lines would have to be tripped. Lastly, note that in all of these results, the total load was served, which demonstrates that it is possible to increase supply reliability without increasing system vulnerability.

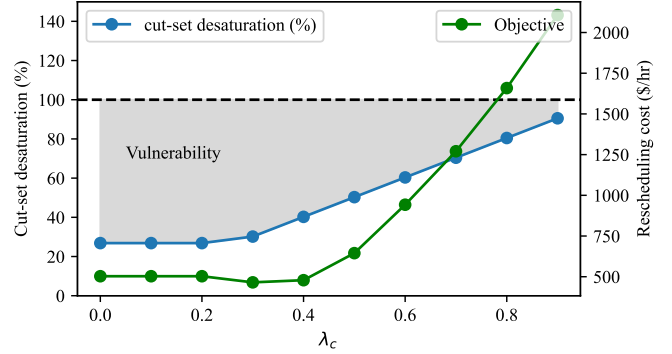


Fig. 5: Sensitivity analysis of the cut-set risk λ_c

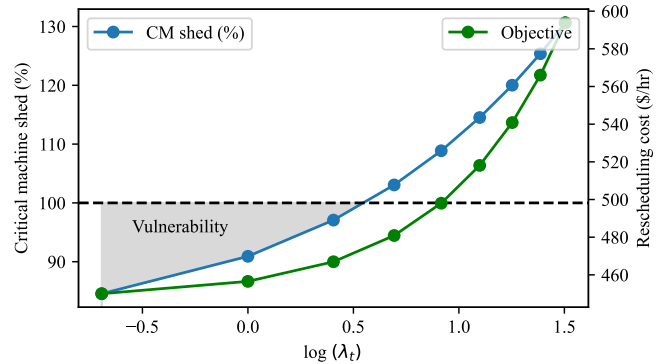


Fig. 6: Sensitivity analysis of the transient stability risk λ_t

V. CONCLUSION

In this paper, a holistic preventive-corrective action scheme addressing both static and dynamic security criteria was introduced that facilitates stability and security-constrained unit commitment/optimal power flow solutions for wildfire-related contingencies. A fast and scalable algorithm for cut-set detection and correction, called FT, is used to analyse extreme event scenarios from a static security perspective. This algorithm is combined with a data-driven linear TSCP model that is able to accurately and reliably predict the appropriate correction factor for mitigating transient instabilities under various loading conditions. A two-stage optimization model is then proposed that utilizes the contingency analyses and enables optimal decision-making in the day-ahead and real-time stages. In the day-ahead stage, the cut-set and stability constrained unit commitment (CSCUC) performs a modified UC considering a post-contingency scenario to determine additional generators to be brought online. In real-time, the cut-set and stability constrained optimal power flow (CSCOPF) is able to determine multiple redispatch solutions based on the current risk of wildfires.

Implementation of the proposed model on the IEEE 118-bus system shows that the FT algorithm and the TSCP model are able to accurately and reliably predict the static and dynamic stability constraints in the face of load uncertainties. The numerical results show that the proposed preventive-corrective coordinated optimization is able to detect and alleviate all cascading outage risks for both lines and generators, while bearing minimal additional operational cost. A comparison with similar models shows that the proposed model is able to achieve security and stability while being fast and economical. With suitable modifications, the proposed formulation can be applied to other extreme event scenarios as well. Future work will pivot towards the synergistic integration of renewable resources, from both economic and physical perspectives (such as ride-through constraints), into the proposed CSCUC/CSCOPF problem formulation.

REFERENCES

- [1] D. A. Z. Vazquez, F. Qiu, N. Fan, and K. Sharp, "Wildfire mitigation plans in power systems: A literature review," *IEEE Transactions on Power Systems*, vol. 37, no. 5, pp. 3540–3551, 2022.
- [2] J. W. Muhs, M. Parvania, and M. Shahidehpour, "Wildfire risk mitigation: A paradigm shift in power systems planning and operation," *IEEE Open Access Journal of Power and Energy*, vol. 7, pp. 366–375, 2020.
- [3] M. Nazemi and P. Dehghanian, "Powering through wildfires: An integrated solution for enhanced safety and resilience in power grids," *IEEE Transactions on Industry Applications*, vol. 58, no. 3, pp. 4192–4202, 2022.
- [4] A. Umunnakwe and K. Davis, "A data-driven automated mitigation approach for resilient wildfire response in power systems," *IEEE Open Access Journal of Power and Energy*, 2023.
- [5] M. Rostamzadeh, M. H. Kapourchali, L. Zhao, and V. Aravinthan, "Optimal reconfiguration of power distribution grids to maintain line thermal efficiency during progressive wildfires," *IEEE Systems Journal*, 2023.
- [6] M. Choobineh, B. Ansari, and S. Mohagheghi, "Vulnerability assessment of the power grid against progressing wildfires," *Fire Safety Journal*, vol. 73, pp. 20–28, 2015. [Online]. Available: <https://www.sciencedirect.com/science/article/pii/S0379711215000168>
- [7] North America Electric Reliability Corporation (NERC), "1,200 MW fault induced solar photovoltaic resource interruption disturbance report," 2016.
- [8] P. Moutis and U. Sriram, "PMU-driven non-preemptive disconnection of overhead lines at the approach or break-out of forest fires," *IEEE Transactions on Power Systems*, vol. 38, no. 1, pp. 168–176, 2023.
- [9] J. J. Macwilliams, J. Kobus, and S. L. Monaca, "PG&E: Market and policy perspectives on the first climate change bankruptcy," 2019.
- [10] A. Arab, A. Khodaei, R. Eskandarpour, M. P. Thompson, and Y. Wei, "Three lines of defense for wildfire risk management in electric power grids: A review," *IEEE Access*, vol. 9, pp. 61 577–61 593, 2021.
- [11] R. Bayani, M. Waseem, S. D. Manshadi, and H. Davani, "Quantifying the risk of wildfire ignition by power lines under extreme weather conditions," *IEEE Systems Journal*, vol. 17, no. 1, pp. 1024–1034, 2023.
- [12] D. L. Donaldson, M. S. Alvarez-Alvarado, and D. Jayaweera, "Integration of electric vehicle evacuation in power system resilience assessment," *IEEE Transactions on Power Systems*, 2022.
- [13] J. Su, S. Mehrani, P. Dehghanian, and M. A. Lejeune, "Quasi second-order stochastic dominance model for balancing wildfire risks and power outages due to proactive public safety de-energizations," *IEEE Transactions on Power Systems*, pp. 1–14, 2023.
- [14] R. Bayani and S. D. Manshadi, "Resilient expansion planning of electricity grid under prolonged wildfire risk," *IEEE Transactions on Smart Grid*, vol. 14, no. 5, pp. 3719–3731, 2023.
- [15] R. S. Biswas, A. Pal, T. Werho, and V. Vittal, "A graph theoretic approach to power system vulnerability identification," *IEEE Transactions on Power Systems*, vol. 36, no. 2, pp. 923–935, 2020.
- [16] R. S. Biswas, A. Pal, T. Werho, and V. Vittal, "Mitigation of saturated cut-sets during multiple outages to enhance power system security," *IEEE Transactions on Power Systems*, vol. 36, no. 6, pp. 5734–5745, 2021.
- [17] M. Abdelmalak and M. Benidris, "Proactive generation redispatch to enhance power system resilience during hurricanes considering unavailability of renewable energy sources," *IEEE Transactions on Industry Applications*, vol. 58, no. 3, pp. 3044–3053, 2022.
- [18] C. Guo, C. Ye, Y. Ding, and P. Wang, "A multi-state model for transmission system resilience enhancement against short-circuit faults caused by extreme weather events," *IEEE Transactions on Power Delivery*, vol. 36, no. 4, pp. 2374–2385, 2021.
- [19] H. Yuan and Y. Xu, "Preventive-corrective coordinated transient stability dispatch of power systems with uncertain wind power," *IEEE Transactions on Power Systems*, vol. 35, no. 5, pp. 3616–3626, 2020.
- [20] J. U. Sevilla-Romero, A. Pizano-Martínez, C. R. Fuerte-Esquivel, and R. Ramírez-Betancour, "Two-stage transient-stability-constrained optimal power flow for preventive control of rotor angle stability and voltage sags," *Journal of Modern Power Systems and Clean Energy*, 2023.
- [21] Y. Xu, Z. Y. Dong, R. Zhang, Y. Xue, and D. J. Hill, "A decomposition-based practical approach to transient stability-constrained unit commitment," *IEEE Transactions on Power Systems*, vol. 30, no. 3, pp. 1455–1464, 2014.
- [22] T. Wu and J. Wang, "Transient stability-constrained unit commitment using input convex neural network," *IEEE Transactions on Neural Networks and Learning Systems*, 2023.
- [23] N. Rhodes, L. Ntaimo, and L. Roald, "Balancing wildfire risk and power outages through optimized power shut-offs," *IEEE Transactions on Power Systems*, vol. 36, no. 4, pp. 3118–3128, 2021.
- [24] C. Haseltine and L. Roald, "The effect of blocking automatic reclosing on wildfire risk and outage times," in *2020 52nd North American Power Symposium (NAPS)*, 2021, pp. 1–6.
- [25] G. N. Lopes, T. S. Menezes, D. P. S. Gomes, and J. C. M. Vieira, "High impedance fault location methods: Review and harmonic selection-based analysis," *IEEE Open Access Journal of Power and Energy*, vol. 10, pp. 438–449, 2023.
- [26] D. P. S. Gomes, C. Ozansoy, and A. Ulhaq, "High-sensitivity vegetation high-impedance fault detection based on signal's high-frequency contents," *IEEE Transactions on Power Delivery*, vol. 33, no. 3, pp. 1398–1407, 2018.
- [27] J. Ma, J. C. Cheng, F. Jiang, V. J. Gan, M. Wang, and C. Zhai, "Real-time detection of wildfire risk caused by powerline vegetation faults using advanced machine learning techniques," *Advanced Engineering Informatics*, vol. 44, p. 101070, 2020.
- [28] H. Daochun, L. Peng, R. Jiangjun, Z. Yafei, and W. Tian, "Review on discharge mechanism and breakdown characteristics of transmission line gap under forest fire condition," *High Voltage Engineering*, vol. 41, no. 2, pp. 622–632, 2015.
- [29] S. Dian, P. Cheng, Q. Ye, J. Wu, R. Luo, C. Wang, D. Hui, N. Zhou, D. Zou, Q. Yu, and X. Gong, "Integrating wildfires propagation prediction into early warning of electrical transmission line outages," *IEEE Access*, vol. 7, pp. 27 586–27 603, 2019.
- [30] "FlamMap," US Forest Service, Rocky Mountain Research Station, Fire, Fuel, and Smoke Science Program, <https://www.firelab.org/project/flammap>, last accessed October 2023.
- [31] H. Yang, N. Rhodes, H. Yang, L. Roald, and L. Ntaimo, "Multi-period power system risk minimization under wildfire disruptions," *IEEE Transactions on Power Systems*, pp. 1–13, 2024.
- [32] M. Abdelmalak and M. Benidris, "Enhancing power system operational resilience against wildfires," *IEEE Transactions on Industry Applications*, vol. 58, no. 2, pp. 1611–1621, 2022.
- [33] Y. Xu, J. Ma, Z. Y. Dong, and D. J. Hill, "Robust transient stability-constrained optimal power flow with uncertain dynamic loads," *IEEE Transactions on Smart Grid*, vol. 8, no. 4, pp. 1911–1921, 2017.
- [34] S. Sahoo and A. Pal, "Cut-set and stability constrained optimal power flow for resilient operation during wildfires," *arXiv preprint arXiv:2311.05734*, 2023.
- [35] A. Malik, M. R. Rao, N. Puppala, P. Koori, V. A. K. Thota, Q. Liu, S. Chiao, and J. Gao, "Data-driven wildfire risk prediction in northern california," *Atmosphere*, vol. 12, no. 1, p. 109, 2021.
- [36] R. S. Allison, J. M. Johnston, G. Craig, and S. Jennings, "Airborne optical and thermal remote sensing for wildfire detection and monitoring," *Sensors*, vol. 16, no. 8, p. 1310, 2016.
- [37] S. Sahoo, A. I. Sifat, and A. Pal, "Data-driven flow and injection estimation in PMU-unobservable transmission systems," in *2023 IEEE Power & Energy Society General Meeting*. IEEE, 2023, pp. 1–5.
- [38] A. B. Birchfield, T. Xu, K. M. Gagner, K. S. Shetye, and T. J. Overbye, "Grid structural characteristics as validation criteria for synthetic networks," *IEEE Transactions on Power Systems*, vol. 32, no. 4, pp. 3258–3265, 2017.